CLIMATE CHANGE

Global exposure risk of frogs to increasing environmental dryness

Nicholas C. Wu[1,*], Rafael Parelli Bovo[2,3], Urtzi Enriquez-Urzelai[4], Susana Clusella-Trullas[5], Michael R. Kearney[6], Carlos A. Navas[2,7], Jacinta D. Kong[8,9]

[1]*Hawkesbury Institute for the Environment, Western S=ydney University, New South Wales 2753, Australia.* [2]*Departmento de Fisiologia, Instituto de Biociências, Universidade de São Paulo, São Paulo 05508090, Brazil.* [3]*Department of Evolution, Ecology, and Organismal Biology, University of California Riverside, CA, United States.* [4]*Czech Academy of Sciences, Institute of Vertebrate Biology, Květná 8, 60365 Brno, Czech Republic.* [5]*Department of Botany and Zoology & School for Climate Studies, Stellenbosch University, Stellenbosch 7600, South Africa.* [6]*School of BioSciences, The University of Melbourne, Melbourne, Victoria, Australia.* [7]*Edward Bass Distinguished Scholar, YIBS/Ecology & Evolutionary Biology, Yale University, CT, United States.* [8]*School of Natural Sciences, Trinity College Dublin, Dublin 2, Ireland.* [9]*Department of Biology, Carleton University, Ottawa K1S 5B6, Canada*.
*Corresponding author. Email: nicholas.wu.nz@gmail.com

amphibian decline, climate change, dehydration, desiccation, hydroregulation, macrophysiology, thermoregulation

Species exposed to prolonged drying are at risk of population declines or extinctions. Understanding species' sensitivity to water loss and microhabitat preference, or ecotype, is therefore vital for assessing climate change risks. Here, we mapped global areas where water-sensitive vertebrates, i.e., anurans, will face increasing aridity and drought, analysed ecotype sensitivity to water loss, and modelled behavioural activity impacts under future drought and warming scenarios. Predictions indicate 6.6% to 33.6% of anuran habitats will become arid-like by 2080–2100, with 15.4% to 36.1% exposed to worsening drought, under an intermediate to high emission scenario, respectively. Critically, arid conditions are expected to double water loss rates. Biophysical models demonstrated a 11.45 ± 8.95% reduction in anuran activity under combined drought and warming, compared to the 6.74 ± 3.95% reduction from warming alone in the warmest quarter. These findings underscore the pervasive synergistic threat of warming and environmental drying to anurans.

INTRODUCTION

Global warming and land modification are expected to increase the frequency and intensity of droughts, which are anomalous periods of low precipitation [1-3]. This synergistic interaction is accelerating extinction risk for species sensitive to rapid water loss [4,5]. Amphibians are prime examples of terrestrial species that are heavily dependent on water, and often have higher rates of water loss than other terrestrial animals [6,7]. Synthesis studies on the effects of climate change on amphibians [8,9] and global assessments of climate vulnerability show amphibians are highly vulnerable to increasing temperature and heating events [10-13]. Since amphibians are dependent on water, there is a critical need to understand how both temperature and extreme moisture deficit events such as drought will impact amphibians, given their sensitivity to water loss and their threatened status relative to other taxonomic groups [14].

Assessing species vulnerability to environmental drying relies on the degree of exposure and the species' sensitivity to the exposure [15]. The extent of exposure to drying depends on the frequency, intensity, and duration of drought events. However, the impact of environmental drying is not singular [16]. While environmental water stress primarily depends on surrounding water availability (in the air, substrate, and water bodies) and how much is evaporated or transpired by plants [17], warming alone will increase evaporation rates by increasing the vapor pressure deficit (VPD). VPD is one of the primary forces driving evaporation rates and atmospheric drought [18]. High VPDs are known to be major drivers of mortality events in plants [19,20]. The rise in evaporation rates from high VPD reduces activity in many ectotherms [21,22]. Experimental and field studies have suggested amphibians behaviourally prefer environments that maintain hydration over thermoregulation, emphasising the importance of water availability and microrefugia in informing climate vulnerability [23-25]. Understanding water loss vulnerability is therefore a necessary component for determining amphibian vulnerability to global environmental change.

Behavioural and physiological sensitivity to water loss can vary by species accordingly. Frogs display a diversity of natural histories, including specialist ecological types (ecotype) with unique adaptations to drying conditions[26]. Fossorial species burrow underground during the non-breeding period to aestivate [27], with some producing water-proof cocoons to conserve water [28,29]. Some arboreal anurans produce waxy skin secretions that reduce evaporative water loss [30-32]. Most amphibians, however, are more vulnerable to dehydrating conditions compared to other terrestrial vertebrates and must therefore behaviourally maintain water balance by using shade, burrows, or by adopting a water conserving posture when inactive [33]. Consequently, some ecotypes are likely to be more sensitive to environmental drying than others due to the microclimate preferences and limited physiological adaptations to conserve water. The increased intensity, frequency, and duration of drought conditions—even for arid specialists—can impact anurans by restricting the activity periods for foraging, seeking mates, dispersing, and delaying breeding cycles [22,34-36], all of which may ultimately affect population dynamics, disease susceptibility, and geographic distribution [5,37,38].

Water balance is thus important for amphibians, yet assessments of climate vulnerability incorporating water loss and environmental drying have not been made on a global scale. In this study, we aimed to (i) identify regions where anurans are at risk to increased aridity and drought by quantifying the spatial overlap between anuran species richness and areas of increasing aridification and drought (including intensity, frequency and duration) under future warming scenarios, (ii) examine ecotype sensitivity of adult anurans to evaporative water loss and water uptake through comparative meta-analyses, and (iii) simulate physiological limits for activity of a hypothetical adult frog under future drought and warming scenarios in order to assess the relative effects of warming and/or drought on changes in potential activity hours for each water-conserving strategy. We focused on water loss risk for adult terrestrial anurans because most larval stages are aquatic and rely on water bodies.

METHODS

Aridity and drought risk

Global climatic water balance data

The global water cycle is complex, and many indices have been used to understand and predict environmental water stress across space and time [39-41]. Here, we used two common metrices of environmental dryness, the aridity index (AI), and the Palmer Drought Severity Index (PDSI). The AI represents the degree of dryness of the climate and is calculated as the ratio of the total amount of water supply (precipitation) relative to the amount of water loss (potential evapotranspiration). More arid regions have a smaller index value [42]. In this study, the AI represented the broadscale dryness experienced by amphibians in that area. The PDSI is a widely used meteorological drought index calculated using soil moisture and precipitation data of previous months. The PDSI takes into account the basic effect of global warming through potential evapotranspiration by using surface air temperature and a physical water balance model, and is effective in characterising long-term drought [43,44]. In this study, the PDSI represented extreme changes in meteorological water deficit or surplus. The AI was categorised to five categories (Humid, Dry sub-humid, Semi-arid, Arid, and Hyper-arid) and the PDSI was categorised to seven categories (Extremely moist, Very moist, Moderate moist, Normal, Moderate drought, Severe drought, and Extreme drought) based on descriptions from Budyko [45] and Palmer [43] in **Table S1**.

High resolution (~4km^2) global data on precipitation (mm/month) and potential evapotranspiration (mm/month) were obtained from Abatzoglou et al. [46] under 1) the current climate (1970–2000), 2) an intermediate greenhouse gas emission scenario of +2°C (Shared Socioeconomic Pathway 2–4.5; SPP2–4.5), and 3) a high greenhouse gas emission or "business-as-usual" scenario of +4°C (SSP5–8.5) by 2080–2099 (**Fig. S1a–i**). We used a self-calibrated PDSI with Penman–Monteith potential evapotranspiration representing the current climate (1970–2000) and an intermediate and high emission scenario by 2080–2099 (SSP2–4.5 and SSP5-8.5) from Zhao and Dai [2]. The SSP2–4.5 and SSP5–8.5 scenarios were based on the average of 25 Coupled Model Intercomparison Project Phase 6 (CMIP6) models of precipitation, evapotranspiration, soil moisture, and runoff [47], where the mean annual surface temperature is expected to increase by 2.7°C (2.1–3.5°C range) and 4.4°C (3.3–5.7°C range), respectively by 2080–2100 [48]. Zhao and Dai [2] noted that there are large uncertainties in the drought projections. Therefore, our interpretation is based on the average projected drought which is typically in line with other indices of drought [2,39,40,49,50].

Anuran species richness, ecotype, and distribution

We extracted the geographic range (excluding introduced range), and ecological types of all anuran species (6,416 species) on the 11/01/2021 listed in the International Union for Conservation (IUCN) of Nature's Red List of Threatened Species platform [51]. Ecotypes were classified based on IUCN [51] and Moen and Wiens [52] focusing on adult behaviour and microhabitat preferences outside the breeding season given that many anurans breed in water but are not adapted to live in water all year (**Table S2**). Ecotypes were defined to provide generalised microhabitat use and for modelling the activity in different microhabitats. For example, arboreal species regularly access vertical environments like trees and rock crevices, while stream-dwelling species are restricted to permanent streams or flowing water bodies. We acknowledge that ecotype grouping does not capture the diversity of microclimate preferences. Where possible, we included secondary ecotypes in the raw data, but we analysed species based on their primary ecotype. For example, some species that frequents permanent water bodies, but occasionally observed climbing on trees would primarily be classified as 'semi-aquatic' and secondarily as 'arboreal' as they do not spend a substantial amount of time climbing. Species richness was defined as the sum of species in each grid cell (0.5°), based on the geographic range, and was calculated using the 'calcSR' function from the *rasterSp* package (https://github.com/RS-eco/rasterSp). All raster data were examined and visualised at a spatial resolution of 0.5 arc minute.

Species richness with aridity and PDSI

To examine the relationship between species richness and aridity, the number of species per grid cell was overlapped with the aridity raster layer, where each grid cell was assigned an AI category. The change in species richness between the current and projected (either +2 or +4 °C warming) AI category was calculated as the change in AI category grids occupied by anurans relative to the future projection; a lower number indicates a reduced number of species with the assigned AI category and vice versa.

With a monthly prediction of PDSI from 1950 to 2100 globally available from Zhao and Dai [2], we classified future drought risk in three ways: 1) increase in mean drought intensity (change in PDSI or $\Delta PDSI_{[intensity]}$), 2) increase in mean drought frequency (monthly PDSI count below -2 per year or $\Delta PDSI_{[frequency]}$), and 3) increase in mean drought duration (number of consecutive months with PDSI values below -2 or $\Delta PDSI_{[duration]}$). Change in mean $\Delta PDSI_{[intensity]}$, $\Delta PDSI_{[frequency]}$, and $\Delta PDSI_{[duration]}$ under a +2 or +4 °C warming scenario (2080–2100) was calculated relative to the 1970–

2000 monthly climatology per grid cell ($\Delta PDSI = PDSI_{[future]} - PDSI_{[current]}$). Results are presented in the main text as $\Delta PDSI_{[intensity]}$, $\Delta PDSI_{[frequency]}$ and $\Delta PDSI_{[duration]}$ relative to current scenario (1970–2000). The absolute $PDSI_{[intensity]}$, $PDSI_{[frequency]}$ and $PDSI_{[duration]}$ under a +2 or +4 °C warming scenario (2080–2100) are also presented in **Fig. S2a–i**.

The simultaneous risk of increasing drought intensity, frequency, and duration within a grid cell that are occupied by anurans (species assemblages) was calculated by converting each risk category as binary. Grid cells with a $\Delta PDSI_{[intensity]}$ below -2 (indicating increased drought intensity relative to current scenario) were assigned a '1' binary. Both $\Delta PDSI_{[frequency]}$ and $\Delta PDSI_{[duration]}$ were assigned a binary of '1' if the grid cell has a value of 1 month or higher (indicating increase in frequency or duration relative to current scenario). The number of overlapping binaries were summed up per grid cell. Therefore, a risk factor of 2 indicate species assemblages in the grid cell are at increasing risk of two drought events. We estimated which species assemblages were at risk of experiencing drought events using an arbitrary risk factor scale (species richness × drought risk), where grid cells with high drought risk and high species richness have higher "assemblage-level risk" than grid cells with high drought risk and low species richness (low assemblage-level risk).

Ecotype sensitivity

Water loss and uptake data

We systematically reviewed the literature on experimental water loss and uptake studies for adult anurans following the PRISMA-EcoEvo protocol [53]. Full detail of the systematic search, exclusion criteria, and data extraction are presented in the Supplementary Information and visualised in **Fig. S3**. Studies were included if the following hydrological metrics were reported: water loss as the rate of evaporative water loss (EWL), resistance to water loss (total r_t or relative r_i), change in body mass (absolute or relative), and water uptake as the rate of cutaneous water uptake (WU). Water loss measurements either by forced convection (via wind speed manipulation) or free convection (desiccant) were included in the dataset. The rate of EWL typically incorporates cutaneous and respiratory water loss as most studies do not include methods to distinguish the difference between the two routes of water loss. However, respiratory EWL is assumed to contribute little (5.5% at 25 °C) to the total EWL for amphibians [54]. Additionally, the daily turnover of water for a typical amphibian from other processes such as food and water gain, metabolic water production, and urine and faecal loss is considered negligible and equivalent between species for comparative purposes [7], thus we did not consider these aspects when comparing ecotype risk. The rate of EWL, skin resistance (r_i), and cutaneous WU were standardised to a common unit of mg h^{-1}, and s cm^{-1} for relative skin resistance using standard conversions and approximations via biophysical principles (see Supplementary Information section "Calculations and conversions").

We extracted the mean values, variance (either standard deviation or standard error), and sample size from either the study's main text, supplementary text, table, figures via metaDigitize [55], or calculated from the raw data. We also extracted the mean body mass (g), the exposed ambient temperature (°C) during the experiment, skin temperature measured (°C), coordinates of collection site (latitude and longitude in decimal degrees), flow rate (as cm s^{-1} or ml s^{-1}), duration of the experiment (min), the relative humidity (RH; %) and noted whether the animal was in a physiological water-conserving state (e.g., aestivation, cocoon-forming, or water-proof via cutaneous surface fluid or lipids). Dry air from desiccants without RH presented were assumed to be 1% RH. Missing information were obtained by contacting the study authors where possible. We noted if urine was voided prior to the EWL experiments, body mass was defined as "standard body mass" as the presence of urine will affect water loss. Additional unpublished data from 39 species of anurans were included and detailed in the 'Unpublished data' section of the Supplementary Information. Note, while we aimed for a comprehensive and representative dataset, there are geographical biases in anuran water loss and uptake studies, especially around the Amazon, central Africa, and Eurasia with high amphibian richness, but little to no water loss and uptake studies (**Fig. S4**). Data curation was formatted following Schwanz et al. [56].

Unpublished data from Brazil were collected according to the experimental procedures approved by the Ethical Committee in Animal Use (CEUA) of the Biosciences Institute (#0820), affiliated with UNESP, Rio Claro, São Paulo, Brazil. License for animal capture and transport was provided by Instituto Brasileiro do Meio Ambiente e dos Recursos Naturais Renováveis (IBAMA, #29703-1 and 22028-1), and Secretaria do Meio Ambiente – Instituto Florestal (#26018 - 013.054/2011). Unpublished data from South Africa were collected in accordance to Western Cape Nature Permit AAA007-00073-0056, and all experimental procedures were approved by the University of Stellenbosch REC:ACU, Research Ethics Committee: Animal Care and Use (SU-ACUM13-00005).

Phylogenetic data

To account for phylogenetic relatedness in the following Bayesian model to examine ecotype sensitivity to water loss and water uptake, we used the amphibian phylogeny of Jetz and Pyron [57] comprising of 7,238 amphibian species. There were 5,636 species from our dataset that matched the tree, and the remaining species were not available as they were described after 2016. Our dataset includes 87.8% of the currently known anuran species listed in the IUCN Red List database. Polytomies were removed using the function 'multi2di', and branch lengths were estimated using the 'compute.brlen' function from the *ape* package [58]. The generated tree was converted to a phylogenetic relatedness correlation matrix for subsequent analysis.

Water loss and uptake analyses

All models used a No-U-Turn Sampler extension of Hamiltonian Monte Carlo [59] Bayesian procedure implemented in the *R* package *brms* [60] to derive posterior distributions and associated credible intervals (CIs) for the fitted parameters. For all models, we constructed four chains with 5,000 steps per chain, including 2,500-step warm-up periods, hence a total of 10,000 steps were

retained to estimate posterior distributions [i.e., (5,000 – 2,500) × 4 = 10,000]. Adapt delta was set at 0.99 to decrease the number of divergent transitions, and the maximum tree depth was set to 15 when the depth of tree evaluated in each iteration was exceeded. Fixed effects were assigned weakly informative priors following a Gaussian distribution ($\ln\beta_0$ mean = 0, SD = 3) to speed up model convergence, and Student's t prior with three degrees of freedom was used for group-level, hierarchical effects. The degree of convergence of the model was deemed as achieved when the Gelman–Rubin statistics, $\hat{R}$ [61], was 1.

Differences in resistance to water loss (r_i) and WU between ecotypes were examined with the 'brms' function from the *brms* package. We analysed r_i because it represents the most physiologically relevant metric of water loss [62,63]. For the r_i water loss model, we included the natural logarithm transformed body mass (lnMass), VPD (lnVPD), and air flow rate (lnFlow) as additive fixed effects. Study ID, lnMass nested in species, and the phylogenetic correlation matrix were included as group-level effects to account for variance between studies, repeated measures within species, and evolutionary history [64]. For the WU model, the fixed effects were lnMass, treatment temperature, and initial hydration level. Relative humidity was never reported during the WU experiments, thus VPD was replaced with exposure temperature. Group-level effects were the same as for the water loss model. Only ecotypes with five or more recordings were analysed [65]. The R^2_{marginal} and $R^2_{\text{conditional}}$ were calculated from the water loss and WU models using the 'r2_bayes' function from the *performance* package [66], and posterior predictive checks were presented in Supplementary **Fig. S5**. All statistical outcomes are presented as mean posterior estimates ± 95% credible intervals (95% CI). The model results were also visualised in **Fig. S6–7**.

Water loss vulnerability

We estimated the impact of SSP2–4.5 (+2 °C) and SSP5–8.5 (+4 °C) scenarios on EWL globally for a typical 8.7 g frog (geometric mean body mass of the study) using the 'ectotherm' function from the *NicheMapR* package [67] and compared the estimated EWL to the spatial distribution of species richness. We extracted high resolution (~4km^2) global dataset on the mean VPD (kPA month) and mean wind speed (m s^{-1} month) from Abatzoglou et al. [46] under the current climate (1970–2000) and under a +2 and +4°C scenario to estimate EWL under the current and future scenario. Wind speed at ground level (1 cm) was interpolated from the reference height of 10 m and assuming a level surface roughness of 0.15 m in an open landscape (https://mrke.github.io/NicheMapR/inst/doc/microclimate-model-theory-equations).

Effect of environmental warming and drying on behavioural activity

To demonstrate the role of water-conserving strategies on the potential hours for activity, we simulated a hypothetical frog in a subtropic biome (Karawatha reserve, Brisbane, Australia). Brisbane has a record of daily rainfall from 1994–current and this area has experienced drought recently (2017–2019). The aim is to explore the interactions between different climate processes on frog activity rather than reflect realistic changes in the ecosystem. We also note that these simulations can be applied to any terrestrial location in the world with species-specific thermal and hydrological variables.

We used *NicheMapR* to construct a biophysical model of the water, and energy balance of a typical adult frog (8.7 g) from Kearney and Porter [67] and Kearney and Enriquez-Urzelai [68] to test the role of behavioural and physiological regulation on potential activity under different thermal and hydric conditions. The default frog model was based on the leopard frog *Lithobates pipiens* and was applied for all ecotypes because r_i and WU rate did not differ between ecotypes (**Table S3–4**). The model was based on the 'thermodynamic niche' modelling scheme, considering thermodynamic effects on the biophysical landscape (**Fig. S8a**). Three hypothetical frog models with differing water saving strategies were simulated to estimate the influence of behaviour and physiological modification on activity (summarised in **Table S5**): 1) a shade model where the frog can thermo-hydroregulate with shade available (0–90% shade), but is not able to burrow or climb up trees to regulate temperature and hydration (representative of a typical ground-dwelling frog), 2) an arboreal model with water-proof skin (high skin resistance) and the ability to climb trees up to 150 cm high to regulate their body temperature and hydration (representative of arboreal frog), 3) burrowing model where the frog is able to burrow underground to a maximum of 200 cm to regulate body temperature and hydration (representative of fossorial species). Semi-aquatic and stream-dwelling ecotypes were not simulated as they are typically found around permanent water bodies, which allows them to quickly rehydrate; our models focused on activity change under drying conditions.

We simulated the potential hours (in a 24 hour day) active in a year (t_{act}) which represents the suitable thermal and hydric conditions for the animal to move beyond their retreat to either catch prey or find mates [67]. Frogs can be active day or night, even though most are nocturnal, but may shift activity times with climate change. Therefore, we estimated the overall potential activity hours available. While frogs can survive losing up to 50% of their body weight before death [7], locomotor performance declines rapidly around 10–30% loss of water [23,69-71], and toads have been observed to seek shade after losing ~14% of their water mass [72]. Therefore, we used a threshold of 80% of hydrated body mass to stop activity, as locomotion is highly impaired below these conditions.

We simulated t_{act} for the hypothetical frog under four climate conditions, 1) current normal scenario (typical air temperature and rainfall), 2) a current drought scenario (typical air temperature and low rainfall), 3) a warming normal scenario (+4°C only), and 4) a warming drought scenario (+4°C and low rainfall). Vapour pressure was computed from the environmental temperature and humidity values which directly affects EWL in the model (driven by the vapour density gradient between the skin surface and the air), while the simulated soil water potential

influences WU rate [68]. The full detail of model specifications and climate model verification are provided in the Supplementary Information "*NicheMapR*" section and **Fig. S9**.

To test the generality of the effects of warming and drought on activity at different biomes, we examined the impact of the four climate conditions (as above) on t_{act} from three additional representative biomes that anurans are known to occupy and are at risk to increasing environmental drying [73]. This included a tropical biome (Salvador, Brazil) representing a yearly warm, wet climate, a Mediterranean biome (Seville, Spain) representing hot, dry summers with cold, wet winters, and a semi-arid biome (Tankwa Karoo, South Africa) representing yearly thermally-variable, dry climate (**Fig. S10**). The same 8.7 g hypothetical frog was simulated under the same conditions as previous for the subtropic biome (Brisbane, Australia). We assumed the same warming scenario of +4°C and a drought scenario with a 50% reduction in rainfall to allow the sites to be comparable.

RESULTS

Species richness, aridity, and drought risk

Amphibian species richness is inversely correlated with the aridity, where the higher the AI, the fewer amphibian species per grid cell (**Fig. 1a-c**). On average, most species classified as stream-dwellers inhabit wetter regions (mean AI of 1.46 ± 0.62 s.d), while most fossorial species live in drier regions

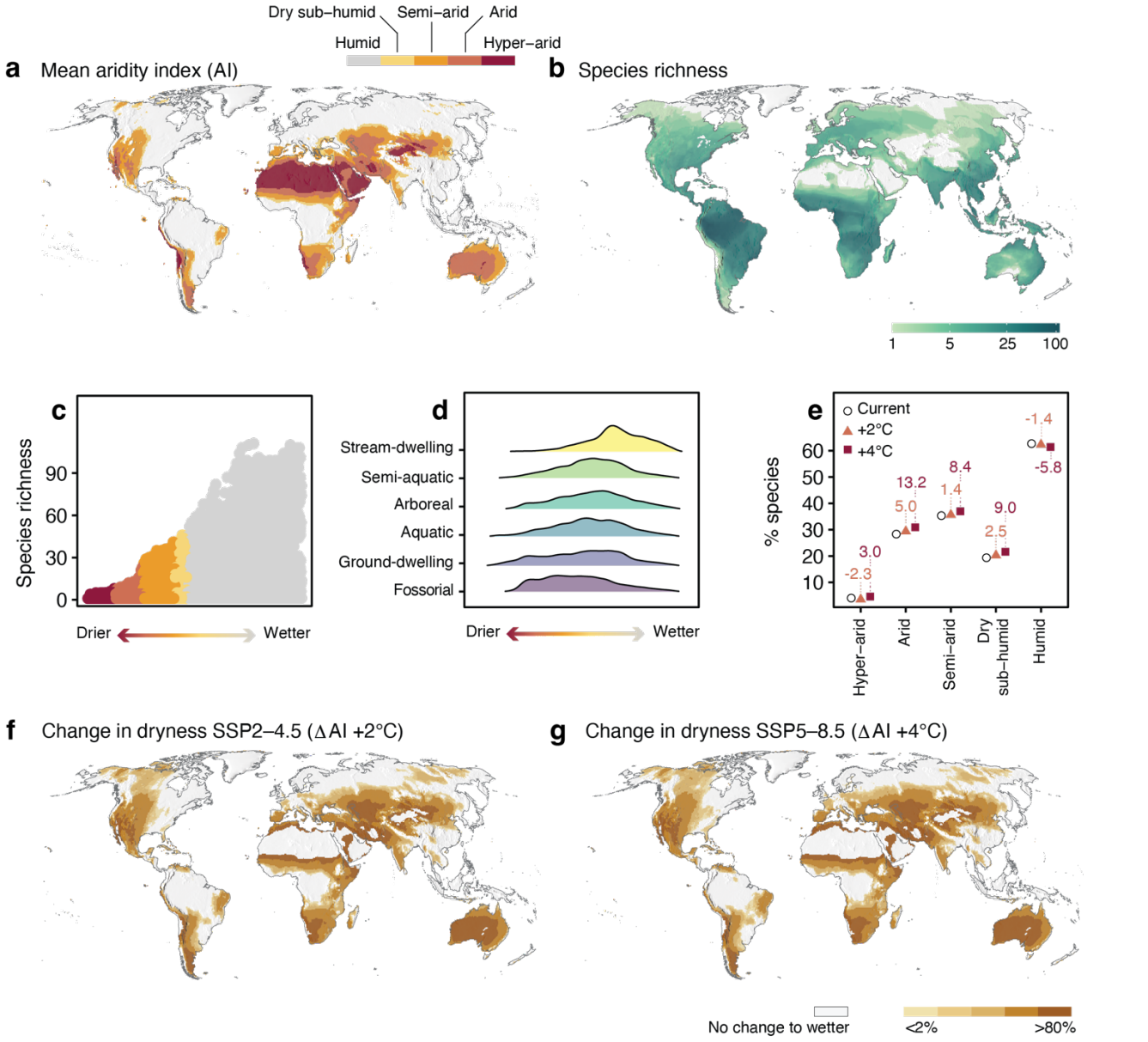

Fig. 1 | Relationship between the spatial distribution of anuran species and the degree of dryness of the climate. **(a)** The spatial distribution of the mean aridity index (AI) based on the precipitation and potential evapotranspiration between 1981–2010, and **(b)** is the anuran species richness based on the IUCN spatial assessment. **(c)** The relationship between mean AI and species richness, where the wetter the climate (lower aridity), the more species richness within the grid cell (0.5°) than drier climates. **(d)** Ecotype-specific distribution of anurans across AI, where stream-dwelling species tend to be conjugated in humid areas, while fossorial species tend to be found in drier areas. **(e)** Change in the percentage of species in each grid cell (0.5°) grouped by AI category between the current climate (yearly average from 1981–2010) and future warming scenario of +2°C (SSP2–4.5) and +4°C (SSP5–8.5) by 2080–2099. Under a +2°C warming scenario, there will be a -1.4 % decrease in percentage of species occupying humid regions and a 6.6% increase in percentage of species occupying drier regions ranging from dry sub-humid to hyper-arid ones. Under a +4°C warming scenario, there will be a -5.8 % decrease in percentage of species occupying humid regions and a 33.6% increase in percentage of species occupying dry sub-humid to hyper-arid regions. **(f–g)** Spatial change in mean dryness (decrease in AI) under a +2°C and +4°C warming scenario.

(mean AI of 0.80 ± 0.61 s.d; **Fig. 1d**). Under an intermediate warming scenario of +2°C, around 6.6% of areas occupied by anurans will increase to arid-like conditions. Humid regions will reduce by 1.4%, dry sub-humid regions will increase by 2.5%, semi-arid regions will increase by 1.4%, arid regions will increase by 5% and hyper-arid regions will decrease by 2.3% (**Fig. 1e** and **1f**). Under a high warming scenario of +4°C, around 33.6% of areas occupied by all anurans will increase to arid-like conditions. Humid regions will reduce by 5.8%, dry sub-humid regions will increase by 9%, semi-arid regions will increase by 8.4%, arid regions will increase by 13.2% and hyper-arid regions will increase by 3% (**Fig. 1e** and **1g**).

By 2080–2100, 15.4 % of regions occupied by anurans are expected to face a combination of increased drought in relation to the three metrics we considered: intensity, frequency, and duration. This is especially so in large areas of South America, northern America, and most of eastern Europe under an intermediate emission scenario (SPP2–4.5; **Fig. 2a**). Under a high emission scenario (SPP5–8.5), 36.1 % of regions occupied by anurans, mainly the Americas, southern Africa, Europe, and southern Australia, will be at risk of increased exposure to drought according to all three metrics (**Fig. 2b**). Anuran species-assemblages in the Amazon region had the highest risk from the combination of high species richness and is predicted to be exposed to increases in all three metrics under both intermediate and high emission scenario (**Fig. 2c–d**).

We estimate around 21% of regions that anurans occupy will be at risk of increasing drought intensity under an intermediate scenario (**Extended Data Fig. 1a–b**). Under a high emission scenario, 38% of the area anurans occupy will be at risk of increasing drought intensity (**Extended Data Fig. 1c–d**). Anurans in central America, southern America, western and central Europe, southern Africa, and southern Australia are expected to be subjected to increased average drought frequency by 1–4 months per year under an intermediate emission scenario (41.1% of areas occupied by anurans; **Extended Data Fig. 2a–b**), while the mean frequency of over 4 months per year are considered rare (0.9%). 15.3% of regions occupied by anurans are expected to reduce in the frequency of drought. Under a high emission scenario, anurans in central America, the Amazon region, Chile, northern United States, and the Mediterranean regions are predicted to experience increases in drought frequency by over 4 months per year (16.3% of areas occupied by amphibians more than 4 months per year; **Extended Data Fig. 2c–d**). 27.4% of regions occupied by anurans are not expected to change and 11% are expected to reduce in drought frequency.

The duration of drought will increase in most of the America's, Europe, southern and central Africa, and southern Australia by 1–4 consecutive months under an intermediate emission scenario (28.6% of areas occupied by anurans; **Extended Data Fig. 3a–b**). The mean durations of over 4 months occurred over a limited area (3.1%). Some areas are expected to experience increases in drought duration by 10 months in the northern United States, Honduras, the Amazon region, Guyana, Chile, Spain, and Türkiye (1.6% of areas occupied by anurans; **Extended Data Fig. 3c–d**).

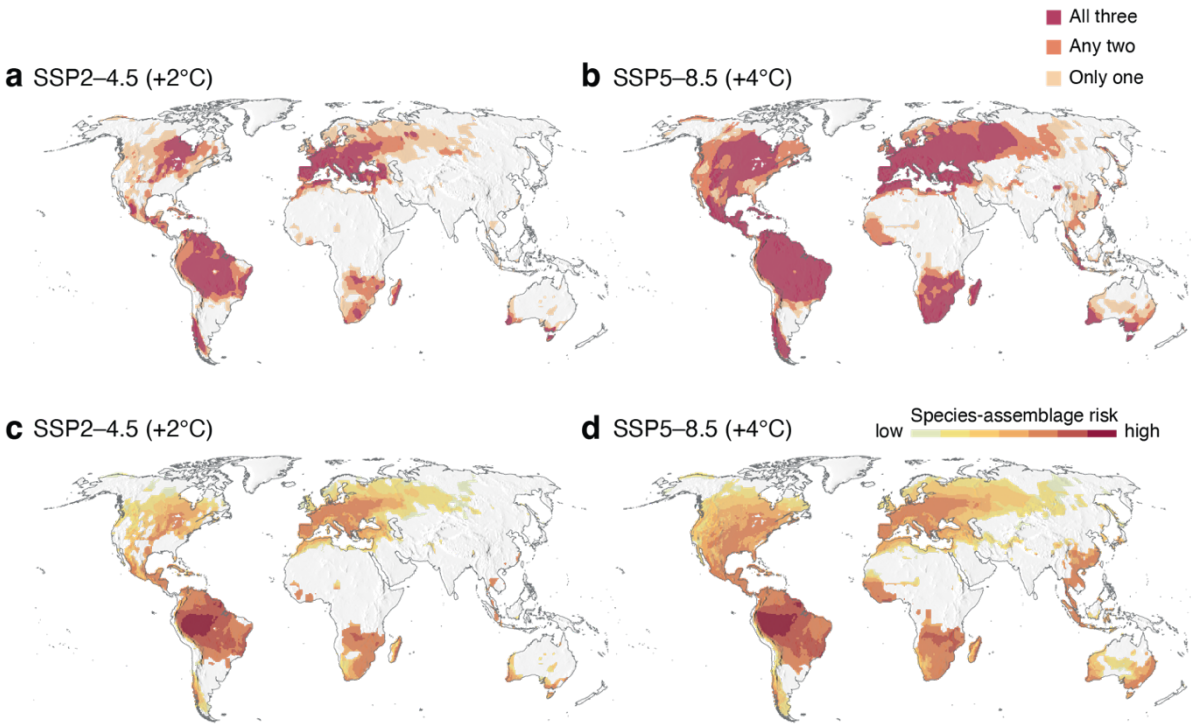

Fig. 2 | Assemblage-level risk due to multiple scenarios of increasing drought events. Grid cells with anuran occurrences exposed to either a single metric (intensity, frequency, or duration: only one), any two metrics (intensity and frequency, frequency and duration, intensity and duration: any two), or all three metrics (intensity, frequency, and duration: all three) of extreme drought events beyond their historic (contemporary) levels by 2080–2100 under **(a)** a +2°C warming scenario (SSP2–4.5) and **(b)** a +4°C warming scenario (SSP5–8.5). The results for drought intensity, frequency, and duration alone are presented in the **Extended Data Figs. 1–3**. **(c–d)** Assemblage-level risk based on the number of drought risk by number of species per grid cell under **(c)** a +2°C warming scenario (SSP2–4.5) and **(d)** a +4°C warming scenario (SSP5–8.5). The drought risk was weighed by species assemblage, where a grid cell with high drought risk and high species richness has a higher risk score than a grid cell with high drought risk and low species richness.

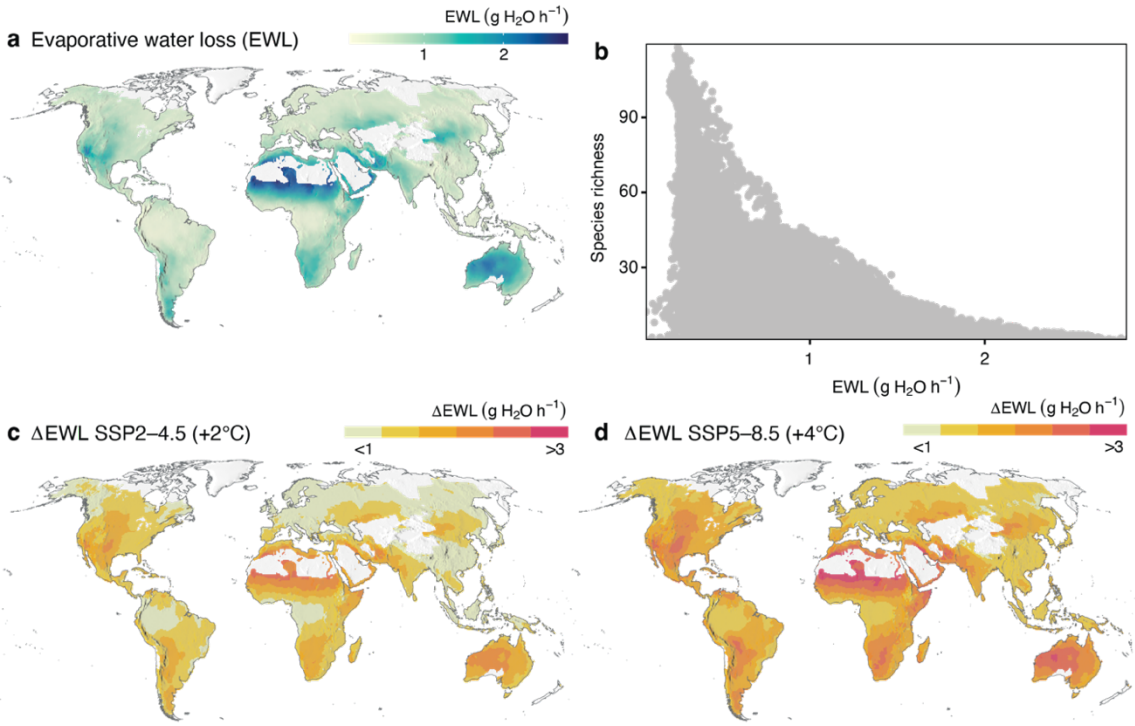

Fig. 3 | Variation in evaporative water loss (EWL) for a typical 8.7 g frog. (a) Spatial variation in EWL (g H_2O h^{-1}) under the current (1981–2010) scenario. **(b)** Relationship between EWL and species richness where the number of species tends to be higher in areas that provide low potential for high EWL (Ecotype specific relationship is presented in **Supplementary Fig. S11**). Bottom maps represent change in EWL (ΔEWL; g H_2O h^{-1}) under **(c)** a +2°C warming scenario (SSP2–4.5) and **(d)** a +4°C warming scenario (SSP5–8.5) by 2080–2100.

Water loss and uptake

Resistance to water loss (r_i) did not differ between ecotypes but varied by water-conserving strategies (**Table S3**; **Fig. S6**). Frogs with water-proof skin (morphological), with a cocoon layer during aestivation (physiological), and inside artificial hollow structures (behavioural) had higher r_i than frogs with no specialised water conserving strategies, with the highest r_i from frogs that were in aestivation (**Fig. S6b**). Body size, and flow rate influenced r_i, which explained 64% [60–68] of the variation in r_i (**Table S3**). r_i increased with body mass with a scaling exponent of 0.10 [0.04–0.17], and higher wind speed decreased r_i (-0.22 [-0.34–-0.10]). There was a moderate phylogenetic signal for r_i (λ = 0.38 [0.04–0.65]). EWL was high for a 8.7 g frog in regions with high annual VPD (indicator of dryness) such as hot, arid regions (**Fig. 3a**). Anuran species richness was negatively related to potential EWL where areas with climates that allow low EWL had a higher number of anuran species (**Fig. 3b**). Under an intermediate and high-emission scenario, EWL increased the most in arid regions (**Fig. 3c-d**), where EWL nearly doubled in the Sahara, Arabian, Taklamakan, and Australian deserts under a high-emission scenario (**Fig. 3d**).

Water uptake did not differ between ecotypes or treatment temperature (**Table S4**). However, water uptake was influenced by body size and initial hydration, both moderators explaining 69% [62–75] of the variation in water uptake. WU increased with body mass with a scaling exponent of 0.80 [0.70–0.91], and more dehydrated frogs had higher water uptake rates (-0.5 [-0.7– -0.04). There was a strong phylogenetic signal for water uptake (λ = 0.78 [0.38–0.94]).

Effect of environmental warming and drying on behavioural activity by ecotype

Biophysical simulations of the current climate scenario (no warming, no drought) in Karawatha Reserve, Australia, showed a hypothetical ground-dwelling frog could be active 3,934 hours out of 8,760 total hours of the year (45%) (**Fig. 4a**). The corresponding values for a water-proof arboreal frog was 4,724 h (54%), and 4,271 h (49%) for a burrowing frog (**Fig. 4c and e**).

Under a warming climate scenario alone (+4 °C, no drought), the ground-dwelling frog increased in potential activity by 334 h (8.5%), the waterproof arboreal frog by 163 h (3.5%), and the burrowing frog by 481 h (8.9%) relative to the current climate scenario. The increase in activity was driven by warmer winters (June to August) allowing for more activity during the coldest quarter (**Fig. 4b, d, g**, **Table S6**). When restricted to the warmest quarter of the year (December to February), where climate warming is predicted to have the greatest impact, warming decreased activity by 8.4% for a ground-dwelling frog, 8.6% for a waterproof frog, and 7.2% for a burrowing frog (**Table S6**).

Under a drought climate scenario (no warming, drought) matching the 2018–2019 historical drought, the ground-dwelling frog decreased potential activity by 205 h (5.2%), the waterproof arboreal frog by 242 h (5.1%), and the burrowing frog by 119 h (2.8%) across the year. The effects of

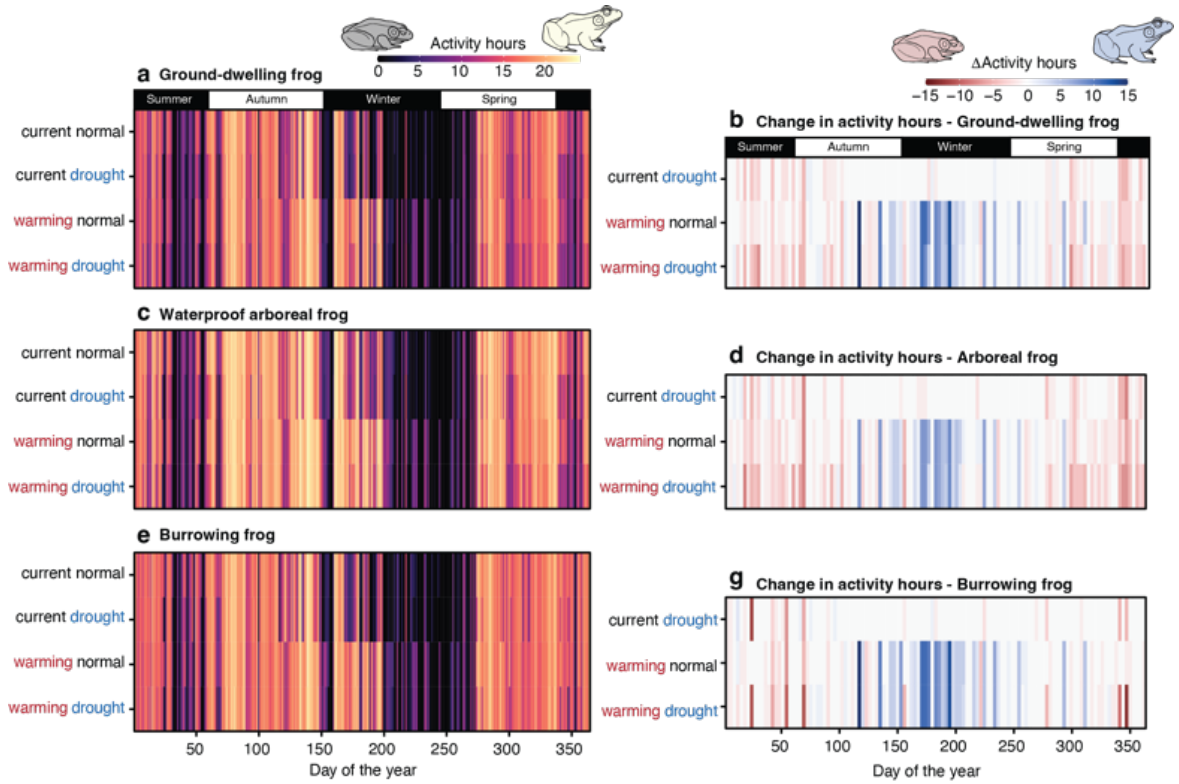

Fig. 4 | Total hours for potential activity and change in activity under different climate conditions for a hypothetical 8.7 g frog in Queensland, Australia. Daily hours of potential activity within suitable thermal and hydric conditions (left panels) and change in activity relative to the current normal scenario (right panels) for **(a-b)** a ground-dwelling frog, **(c-d)** a water-proof arboreal frog, and **(e-g)** a burrowing frog. Total potential activity represented as numbers presented in Supplementary Table S6.

drought were highest in the warmest quarter with an average reduction in potential activity for all ecotypes by 11.2 ± 4.1% relative to the current scenario (**Table S6**). When simulating both warming and drought climate scenarios together, the ground-dwelling frog decreased its potential activity by 221 h (21.8% reduction), the waterproof arboreal frog by 262 h (22.8%), and the burrowing frog by 155 h (12.8%) relative to the current scenario in the warmest quarter. For all ecotypes, a reduction in rainfall had a greater effect on yearly activity than an increase in temperature alone (**Table S6**).

Effect of environmental warming and drying on behavioural activity by biome

Biophysical simulations of a hypothetical ground-dwelling frog under the current scenario could be active in 5,561 hours out of 8,760 total hours of the year (62.5%) in the tropical biome, 42 hours (0.5%) in the semi-arid biome and 372 hours (4.3%) in the Mediterranean biome (**Table S7**). Each biome showed different response in t_{act} under each climate scenarios (**Fig. 5**). The tropical biome showed a decrease in t_{act} for all scenarios across the year (**Fig. 5a**), where warming alone decreased t_{act} by 3.4%, drought alone decreased t_{act} by 21.7%, and the combination of warming and drought decreased t_{act} by 26% (**Table S7**). In the Mediterranean biome, t_{act} increased by 535 h under a warming scenario, while both warming and drought increased t_{act} by 213 h relative to the current scenario (**Table S7**). The increase in t_{act} was driven by increased temperature in the coldest quarter of the year, permitting activity (**Fig. 5b**). t_{act} also showed the same trend in the semi-arid biome (**Fig. 5c**), where t_{act} increased by 37 h under a warming scenario, while both warming and drought increases t_{act} by 35 h relative to the current scenario. However, if restricted to the warmest quarter of the year, activity decreased under all scenarios for all biomes. Warming alone decreased t_{act} by 6.74 ± 3.95%, drought alone decreased t_{act} by 5.5 ± 10.8%, and the combination of warming and drought decreased t_{act} by 11.45 ± 8.95%.

DISCUSSION

Amphibians are the most threatened class of vertebrates, and the number of species directly impacted by climate change has increased by 39% over the last decade [14]. We found the exposure risk of anurans to increasing environmental dryness is global with most regions where anurans live increasing in the average aridity and in the intensity, frequency, and duration of extreme drought events. The Amazon rainforest in South America is of particular concern because high species diversity overlaps with high risk of increasing drought. We also found that sensitivity to water loss vary among species, being driven more by behaviour and physiological adaptations than by ecotypes, and we discuss these findings in the light of responses to warming and drying scenarios. Our results demonstrated how combining the effects of temperature and environmental dryness on the biology and ecology of anurans provides a more comprehensive understanding of the vulnerability of the most threatened vertebrates to climate change.

Stream-dwelling or semi-aquatic ecotypes are expected to have a greater risk of desiccation stress than arboreal or fossorial ecotypes due to differences in adaptation to differing water exposure in their environment. However, the similarities we found in rates of water loss (or skin resistance, r_i) and gain across all ecotypes (**Fig. S6–7**), regardless of phylogeny, suggest that habitat preference does not drive variation in water loss and gain as found in previous studies [74-77]. Instead, a species' risk of desiccation stress may be more tightly related to physiological and behavioural traits. For example, some arboreal species have lower rates of EWL due to their high r_i than other ecotypes. This high r_i may be attributed to either secretions (mucus, lipids, proteins) or specialised cells (iridophores) [6] that allow some "waterproof" species to have r_i values as high as squamates, turtles, and crocodilians [7]. Nevertheless, most anuran species (apart from waterproof and cocoon-forming frogs) lack physiological ways to reduce EWL. Such species must therefore rely on behavioural hydroregulation such as microhabitat shelter to reduce dehydration risk [78-80], otherwise, it is expected that EWL may double in more arid-like regions under a high-emission scenario (**Fig. 3d**). This may be due to arid regions typically subjected to most frequent and intense heatwaves where the spatial extent of extreme thermal events tend to overlap with increasing drought episodes [13], thus exacerbating dehydration.

Arid regions tend to have few, if any, anuran species, and these areas have been expanding to the expense of conserved areas worldwide in part through human activity which can intensify climate changes [48]. This is the case for tropical regions of serious concern, such as Amazon borders and southeast Asia that harbor high species richness and may experience extreme warming and drought [84,85]. The combined effects drought and warming may act synergistically on physiological functions in ways that further reduce potential activity–and perhaps survival–as indicated in our simulated model for a tropical biome (**Fig. 5a**). For example, anurans subjected to drying conditions tend to decrease their thermal tolerance and preferred body temperature [23,81,82], which may lead to suboptimal physiological functions. Additionally, the negative effects of high temperature on frog locomotor performance is exacerbated by dehydration [83,84]. Amphibians will thermoregulate via EWL cooling when exposed to high air temperatures (40–50°C); in such conditions, they can maintain a skin surface temperature around 35°C, but at a

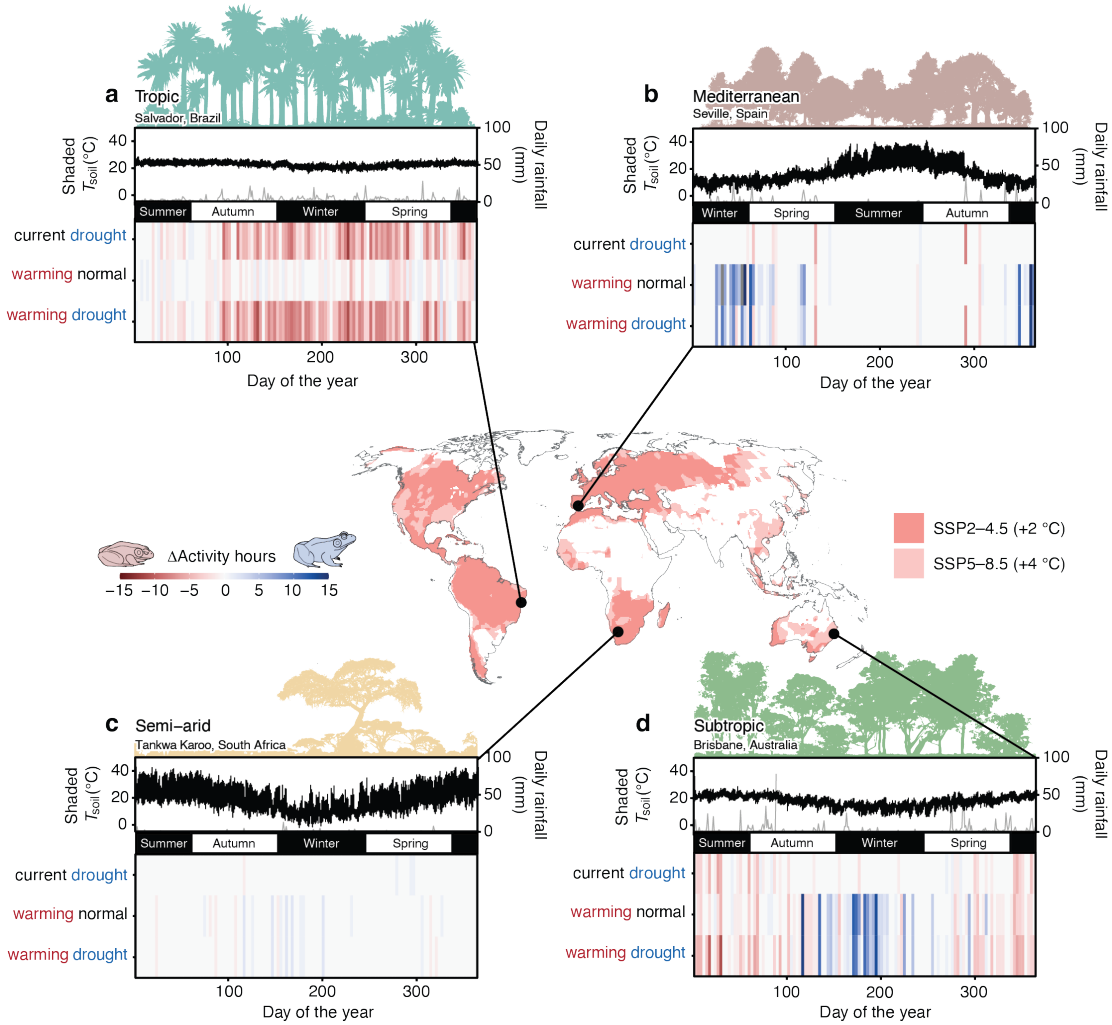

Fig. 5 | Change in activity under different climate conditions for a hypothetical 8.7 g frog in four representative biomes expected to increase in environmental drying. (a) Activity decreased under both warming and drought scenarios in a tropical biome in Brazil across the year. **(b)** Activity increased during the winter months in a Mediterranean biome in Spain. **(c)** Activity slightly decreased in a semi-arid biome in South Africa despite overall low daily potential activity (Supplementary Table S7). **(d)** Activity increased during the winter months and decreased during the summer months in a subtropical biome in Australia. Top graphs for each biome figure show the daily soil temperature in the shade (T_{soil} °C, black lines) and daily rainfall (mm; grey lines), Total potential activity and relative change represented as numbers for each biome are presented in Supplementary Table S7.

cost of increased EWL (**Fig. S11**) and energetic demands [62]. These warming and drying conditions highlight their potential negative impacts on activity and survival of anurans. Indeed, extreme atmospheric evaporative demand under rising temperatures and less predictable rainfall have already been impacting the phenology as well as general biology of terrestrial organisms that depend on water, thus emphasising that the interactions of water and temperature must be considered for accurate forecasting of physiological vulnerability to climate change [16,22].

Physiological-based restrictions on activity, such as of the dehydration effects on movement behaviour, are also of ecological relevance because such effects can limit the ability of organisms to disperse [85], and shorten the time window for breeding [86]. The reduction in activity when dehydrated is likely due to a combination of deceased blood flow and oxygen transport [87,88], brain function [89], and a decline in ability to synthesise ATP and increase in glycolysis during locomotion under water stress [90]. In this sense, environmental drying may not only reduce foraging and mate-seeking opportunities, but may also reduce the environmental resource available to fuel locomotion. Environmental aridity is highly correlated with primary productivity and, ultimately, food availability [91,92]. Thus, environmental drying restricts both the quantity of available food as well as the capacity to find it [22], consequently impairing a number of biological processes associated with activity time. Due to the paucity of amphibian studies directly linking environmental drying and activity in the field [93], our understanding of amphibian sensitivity would benefit from field research focused on species-specific changes in activity in regions to be most at risk to drying as indicated in our study.

Our biophysical simulations indicated a potential decrease in activity hours during the summer period under a warming and drought scenario in all biomes. Conversely, simulations also showed potential increased activity hours during the coldest quarter of the year (more suitable temperatures), which increased the total activity across the year, being even more predominated in biomes with cooler, wet winters such as the subtropic and Mediterranean biomes. As many frogs show plasticity in their call phenology [94,95], it is plausible that some species may change their breeding activity seasonally in response to climate warming. However, responses to changes in water availability during breeding and in winter conditions seems to be species-specific [96], which cautions the generality of species responses to new scenarios of climate change [97] as suggested by our simulations on activity time.

Physiological plasticity can increase an organism's resilience to climate change [98]. Whether amphibians can adapt to increasing environmental dryness will depend on their acclimation capacity. Previous research have indicated amphibians acclimation to drier conditions by increased skin resistance [99], and regenerated capillary beds in the skin [100] which help increased rehydration capacity. Whether these changes permit longer activity under drier conditions, as observed in insects, requires further investigation, especially for small, narrowly distributed species [101,102]. Field observations have shown the average body size in frog assemblages are larger in warmer, drier regions [103-106]. Larger frogs have proportionally lower EWL and have higher water storing capacity in the bladder compared to smaller frogs [7]. Therefore, we may observe phenotypic change in amphibian communities, where larger species may be able to cope better with increased environmental drying relative to smaller species. This contrasts with the third universal response to warming, the declining body sizes [107-109]. Consideration of plasticity is important for evaluating species risk to climate change because plasticity can often, but not always, buffer the effects of environmental stressors [110], and not accounting for plasticity and evolutionary potential can overestimate the impacts of environmental change on predicting species distributions [111,112].

To understand and manage the effects of climate change on biodiversity we must integrate knowledge on biologically relevant processes for different types of organism in different habitats. Hydrological variables such as rainfall, evapotranspiration, soil moisture content have higher uncertainty relative to temperature trends due to the stochastic nature of atmospheric processes [113]. Nonetheless, the growing availability of independent hydrological models provides the perfect opportunity to integrate thermal and hydric constraints to give a deeper understanding of the risk of climate change on other terrestrial organisms than single variables alone.

REFERENCES

1 Pokhrel, Y. *et al.* Global terrestrial water storage and drought severity under climate change. *Nat. Clim. Change* **11**, 226-233 (2021).
2 Zhao, T. & Dai, A. CMIP6 model-projected hydroclimatic and drought changes and their causes in the twenty-first century. *J. Clim.* **35**, 897-921 (2022).
3 Slette, I. J. *et al.* How ecologists define drought, and why we should do better. *Glob. Chang. Biol.* **25**, 3193-3200 (2019).
4 Lowe, W. H., Martin, T. E., Skelly, D. K. & Woods, H. A. Metamorphosis in an era of increasing climate variability. *Trends Ecol. Evol.* **36**, 360-375 (2021).
5 Zylstra, E. R., Swann, D. E., Hossack, B. R., Muths, E. & Steidl, R. J. Drought-mediated extinction of an arid-land amphibian: insights from a spatially explicit dynamic occupancy model. *Ecol. Appl.* **29**, e01859 (2019).
6 Lillywhite, H. B. Water relations of tetrapod integument. *J. Exp. Biol.* **209**, 202-226 (2006).
7 Hillman, S. S., Withers, P. C., Drewes, R. C. & Hillyard, S. D. *Ecological and environmental physiology of amphibians*. Vol. 1 (Oxford University Press 2009).
8 Li, Y., Cohen, J. M. & Rohr, J. R. Review and synthesis of the effects of climate change on amphibians. *Integr. Zool.* **8**, 145-161 (2013).
9 Campbell Grant, E. H., Miller, D. A. & Muths, E. A synthesis of evidence of drivers of amphibian declines. *Herpetologica* **76**, 101-107 (2020).
10 Snyder, G. K. & Weathers, W. W. Temperature adaptations in amphibians. *Am. Nat.* **109**, 93-101 (1975).
11 Gunderson, A. R. & Stillman, J. H. Plasticity in thermal tolerance has limited potential to buffer ectotherms from global warming. *Proc. R. Soc. B. Biol. Sci.* **282**, 20150401 (2015).
12 Pottier, P. *et al.* Vulnerability of amphibians to global warming. *EcoEvoRxiv*, doi:https://doi.org/10.32942/X2T02T (2024).
13 Murali, G., Iwamura, T., Meiri, S. & Roll, U. Future temperature extremes threaten land vertebrates. *Nature* **615**, 461–467 (2023).
14 Luedtke, J. A. *et al.* Ongoing declines for the world's amphibians in the face of emerging threats. *Nature* **622**, 308–314 (2023).
15 Williams, S. E., Shoo, L. P., Isaac, J. L., Hoffmann, A. A. & Langham, G. Towards an integrated framework for assessing the vulnerability of species to climate change. *PLoS Biol.* **6**, e325 (2008).

16 Rozen-Rechels, D. *et al.* When water interacts with temperature: ecological and evolutionary implications of thermo-hydroregulation in terrestrial ectotherms. *Ecol. Evol.* **9**, 10029-10043 (2019).
17 Trenberth, K. E. *et al.* Global warming and changes in drought. *Nat. Clim. Change* **4**, 17-22 (2014).
18 Park Williams, A. *et al.* Temperature as a potent driver of regional forest drought stress and tree mortality. *Nat. Clim. Change* **3**, 292-297 (2013).
19 Grossiord, C. *et al.* Plant responses to rising vapor pressure deficit. *New Phytol.* **226**, 1550-1566 (2020).
20 Eamus, D., Boulain, N., Cleverly, J. & Breshears, D. D. Global change-type drought-induced tree mortality: vapor pressure deficit is more important than temperature per se in causing decline in tree health. *Ecol. Evol.* **3**, 2711-2729 (2013).
21 Kearney, M. R., Munns, S. L., Moore, D., Malishev, M. & Bull, C. M. Field tests of a general ectotherm niche model show how water can limit lizard activity and distribution. *Ecol. Monogr.* **88**, 672-693 (2018).
22 Lertzman-Lepofsky, G. F., Kissel, A. M., Sinervo, B. & Palen, W. J. Water loss and temperature interact to compound amphibian vulnerability to climate change. *Glob. Chang. Biol.* **26**, 4868-4879 (2020).
23 Anderson, R. C. & Andrade, D. V. Trading heat and hops for water: dehydration effects on locomotor performance, thermal limits, and thermoregulatory behavior of a terrestrial toad. *Ecol. Evol.* **7**, 9066-9075 (2017).
24 Galindo, C., Cruz, E. & Bernal, M. Evaluation of the combined temperature and relative humidity preferences of the Colombian terrestrial salamander *Bolitoglossa ramosi* (Amphibia: Plethodontidae). *Can. J. Zool.* **96**, 1230-1235 (2018).
25 Navas, C. A., Antoniazzi, M. M., Carvalho, J. E., Suzuki, H. & Jared, C. Physiological basis for diurnal activity in dispersing juvenile *Bufo granulosus* in the Caatinga, a Brazilian semi-arid environment. *Comp. Biochem. Physiol. Part A Mol. Integr. Physiol.* **147**, 647-657 (2007).
26 Toledo, R. & Jared, C. Cutaneous adaptations to water balance in amphibians. *Comp. Biochem. Physiol. Part A Physiol.* **105**, 593-608 (1993).
27 Carvalho, J. E., Navas, C. A. & Pereira, I. C. in *Aestivation: molecular and physiological aspects* (eds Carlos A Navas & José E Carvalho) 141-169 (Springer, 2010).
28 Withers, P. C. Cocoon formation and structure in the estivating Australian desert frogs, *Neobatrachus* and *Cyclorana*. *Aust. J. Zool.* **43**, 429-441 (1995).
29 Tracy, C. R., Reynolds, S. J., McArthur, L., Tracy, C. R. & Christian, K. A. Ecology of aestivation in a cocoon-forming frog, *Cyclorana australis* (Hylidae). *Copeia* **2007**, 901-912 (2007).
30 Amey, A. P. & Grigg, G. C. Lipid-reduced evaporative water loss in two arboreal hylid frogs. *Comp. Biochem. Physiol. Part A Physiol.* **111**, 283-291 (1995).
31 Stinner, J. N. & Shoemaker, V. H. Cutaneous gas exchange and low evaporative water loss in the frogs *Phyllomedusa sauvagei* and *Chiromantis xerampelina*. *J. Comp. Physiol. B* **157**, 423-427 (1987).
32 Shoemaker, V. H. & McClanahan, L. L. Nitrogen excretion and water balance in amphibians of Borneo. *Copeia* **3**, 446-451 (1980).
33 Pough, F. H., Taigen, T. L., Stewart, M. M. & Brussard, P. F. Behavioral modification of evaporative water loss by a Puerto Rican frog. *Ecology* **64**, 244-252 (1983).
34 Sodhi, N. S. *et al.* Measuring the meltdown: drivers of global amphibian extinction and decline. *PloS one* **3**, e1636 (2008).
35 Ficetola, G. F. & Maiorano, L. Contrasting effects of temperature and precipitation change on amphibian phenology, abundance and performance. *Oecologia* **181**, 683-693 (2016).
36 Wassens, S., Walcott, A., Wilson, A. & Freire, R. Frog breeding in rain-fed wetlands after a period of severe drought: implications for predicting the impacts of climate change. *Hydrobiologia* **708**, 69-80 (2013).
37 Kohli, A. K. *et al.* Disease and the drying pond: examining possible links among drought, immune function, and disease development in amphibians. *Physiol. Biochem. Zool.* **92**, 339-348 (2019).
38 Kupferberg, S. J. *et al.* Seasonal drought and its effects on frog population dynamics and amphibian disease in intermittent streams. *Ecohydrology* **15**, e2395 (2022).
39 Li, H. *et al.* Drylands face potential threat of robust drought in the CMIP6 SSPs scenarios. *Environ. Res. Lett.* **16**, 114004 (2021).
40 Ukkola, A. M., De Kauwe, M. G., Roderick, M. L., Abramowitz, G. & Pitman, A. J. Robust future changes in meteorological drought in CMIP6 projections despite uncertainty in precipitation. *Geophys. Res. Lett.* **47**, e2020GL087820 (2020).
41 Spinoni, J. *et al.* Future global meteorological drought hot spots: A study based on CORDEX data. *J. Clim.* **33**, 3635-3661 (2020).
42 Cherlet, M. *et al. World atlas of desertification*. ed. 3 edn, (Publication Office of the European Union, 2018).
43 Palmer, W. C. *Meteorological drought*. Vol. 30 (US Department of Commerce, Weather Bureau, 1965).
44 Dai, A., Trenberth, K. E. & Qian, T. A global dataset of Palmer Drought Severity Index for 1870–2002: relationship with soil moisture and effects of surface warming. *J. Hydrometeorol.* **5**, 1117-1130 (2004).
45 Budyko, M. I. The heat balance of the earth's surface. *Soviet Geography* **2**, 3-13 (1961).
46 Abatzoglou, J. T., Dobrowski, S. Z., Parks, S. A. & Hegewisch, K. C. TerraClimate, a high-resolution global dataset of monthly climate and climatic water balance from 1958–2015. *Scientific data* **5**, 170191 (2018).
47 Eyring, V. *et al.* Overview of the Coupled Model Intercomparison Project Phase 6 (CMIP6) experimental design and organization. *Geosci. Model Dev.* **9**, 1937-1958 (2016).
48 IPCC. Climate Change 2021: The Physical Science Basis, Contribution of Working Group I to the Sixth Assessment Report of the Intergovernmental Panel on Climate Change. (Cambridge, UK, 2021).
49 Cook, B. I. *et al.* Megadroughts in the common era and the Anthropocene. *Nat. Rev. Earth Environ.* **3**, 741-757 (2022).
50 Qing, Y. *et al.* Accelerated soil drying linked to increasing evaporative demand in wet regions. *npj Clim. Atmos. Sci.* **6**, 205 (2023).
51 IUCN. The IUCN Red List of threatened species. Version 2022-2 (2022). <https://www.iucnredlist.org/>.
52 Moen, D. S. & Wiens, J. J. Microhabitat and climatic niche change explain patterns of diversification among frog families. *Am. Nat.* **190**, 29-44 (2017).
53 O'Dea, R. E. *et al.* Preferred reporting items for systematic reviews and meta-analyses in ecology and evolutionary biology: a PRISMA extension. *Biol. Rev.* **96**, 1695-1722 (2021).
54 Senzano, L. M. & Andrade, D. V. Temperature and dehydration effects on metabolism, water uptake and the partitioning between respiratory and cutaneous evaporative water loss in a terrestrial toad. *J. Exp. Biol.* **221**, jeb188482 (2018).
55 Pick, J. L., Nakagawa, S. & Noble, D. W. Reproducible, flexible and high-throughput data extraction from primary literature: the metaDigitise R package. *Method. Ecol. Evol.* **10**, 426-431 (2019).
56 Schwanz, L. E. *et al.* Best practices for building and curating databases for comparative analyses. *J. Exp. Biol.* **225**, jeb243295 (2022).
57 Jetz, W. & Pyron, R. A. The interplay of past diversification and evolutionary isolation with present imperilment across the amphibian tree of life. *Nat. Eco. Evol.* **2**, 850-858 (2018).
58 Paradis, E. & Schliep, K. ape 5.0: an environment for modern phylogenetics and evolutionary analyses in R. *Bioinformatics* **35**, 526-528 (2018).
59 Hoffman, M. D. & Gelman, A. The No-U-Turn sampler: adaptively setting path lengths in Hamiltonian Monte Carlo. *J. Mach. Learn. Res.* **15**, 1593-1623 (2014).
60 Bürkner, P.-C. brms: an R package for Bayesian multilevel models using Stan. *J. Stat. Softw.* **80**, 1-28 (2017).
61 Gelman, A. & Rubin, D. B. Inference from iterative simulation using multiple sequences. *Stat. Sci.* **7**, 457-472 (1992).
62 Feder, M. E. & Burggren, W. W. *Environmental physiology of the amphibians*. (University of Chicago Press, 1992).
63 Riddell, E. A., Apanovitch, E. K., Odom, J. P. & Sears, M. W. Physical calculations of resistance to water loss improve predictions of species range models. *Ecol. Monogr.* **87**, 21-33 (2017).
64 Pottier, P. *et al.* New horizons for comparative studies and meta-analyses. *Trends Ecol. Evol.* (2024).
65 Nakagawa, S., Noble, D. W., Senior, A. M. & Lagisz, M. Meta-evaluation of meta-analysis: ten appraisal questions for biologists. *BMC biology* **15**, 1-14 (2017).
66 Lüdecke, D., Ben-Shachar, M. S., Patil, I., Waggoner, P. & Makowski, D. performance: an R package for assessment, comparison and testing of statistical models. *J. Open Source Softw.* **6**, 3139 (2021).
67 Kearney, M. R. & Porter, W. P. NicheMapR–an R package for biophysical modelling: the ectotherm and Dynamic Energy Budget models. *Ecography* **43**, 85-96 (2020).

68 Kearney, M. R. & Enriquez-Urzelai, U. A general framework for jointly modelling thermal and hydric constraints on developing eggs. *Method. Ecol. Evol.* **14**, 583-595 (2023).
69 Greenberg, D. A. & Palen, W. J. Hydrothermal physiology and climate vulnerability in amphibians. *Proc. R. Soc. B.* **288**, 20202273 (2021).
70 Beuchat, C. A., Pough, F. H. & Stewart, M. M. Response to simultaneous dehydration and thermal stress in three species of Puerto Rican frogs. *J. Comp. Physiol. B* **154**, 579-585 (1984).
71 Titon Jr, B., Navas, C. A., Jim, J. & Gomes, F. R. Water balance and locomotor performance in three species of neotropical toads that differ in geographical distribution. *Comp. Biochem. Physiol. Part A Mol. Integr. Physiol.* **156**, 129-135 (2010).
72 Bartelt, P. E. *A biophysical analysis of habitat selection in western toads (Bufo boreas) in southeastern Idaho* PhD thesis, Idaho State University, (2000).
73 Christian, J. I. *et al.* Global projections of flash drought show increased risk in a warming climate. *Commun. Earth Environ* **4**, 165 (2023).
74 Thorson, T. B. The relationship of water economy to terrestrialism in amphibians. *Ecology* **36**, 100-116 (1955).
75 Katz, U. & Graham, R. Water relations in the toad (*Bufo viridis*) and a comparison with the frog (*Rana ridibunda*). *Comp. Biochem. Physiol. Part A Physiol.* **67**, 245-251 (1980).
76 Withers, P. C., Hillman, S. S. & Drewes, R. C. Evaporative water loss and skin lipids of anuran amphibians. *J. Exp. Zool.* **232**, 11-17 (1984).
77 Wygoda, M. L. Low cutaneous evaporative water loss in arboreal frogs. *Physiol. Zool.* **57**, 329-337 (1984).
78 de Andrade, D. V. & Abe, A. S. Evaporative water loss and oxygen uptake in two casque-headed tree frogs, *Aparasphenodon brunoi* and *Corythomantis greeningi* (Anura, Hylidae). *Comp. Biochem. Physiol. Part A Physiol.* **118**, 685-689 (1997).
79 Schwarzkopf, L. & Alford, R. Desiccation and shelter-site use in a tropical amphibian: comparing toads with physical models. *Funct. Ecol.* **10**, 193-200 (1996).
80 Seebacher, F. & Alford, R. A. Shelter microhabitats determine body temperature and dehydration rates of a terrestrial amphibian (*Bufo marinus*). *J. Herpetol.* **36**, 69-75 (2002).
81 Mitchell, A. & Bergmann, P. J. Thermal and moisture habitat preferences do not maximize jumping performance in frogs. *Funct. Ecol.* **30**, 733-742 (2016).
82 Guevara-Molina, E. C., Gomes, F. R. & Camacho, A. Effects of dehydration on thermoregulatory behavior and thermal tolerance limits of *Rana catesbeiana* (Shaw, 1802). *J. Therm. Biol.* **93**, 102721 (2020).
83 Preest, M. & Pough, F. H. Interaction of temperature and hydration on locomotion of toads. *Funct. Ecol.* **3**, 693-699 (1989).
84 Walvoord, M. E. Cricket frogs maintain body hydration and temperature near levels allowing maximum jump performance. *Physiol. Biochem. Zool.* **76**, 825-835 (2003).
85 Wu, N. C. & Seebacher, F. Physiology can predict animal activity, exploration, and dispersal. *Comm. Biol.* **5**, 1-11 (2022).
86 Wassens, S., Walcott, A., Wilson, A. & Freire, R. Frog breeding in rain-fed wetlands after a period of severe drought: implications for predicting the impacts of climate change. *Hydrobiologia* **708**, 69-80 (2013).
87 Hillman, S. S. Dehydrational effects on cardiovascular and metabolic capacity in two amphibians. *Physiol. Zool.* **60**, 608-613 (1987).
88 Hillman, S. S. The roles of oxygen delivery and electrolyte levels in the dehydrational death of *Xenopus laevis*. *J. Comp. Physiol.* **128**, 169-175 (1978).
89 Hillman, S. S. Dehydrational effects on brain and cerebrospinal fluid electrolytes in two amphibians. *Physiol. Zool.* **61**, 254-259 (1988).
90 Gatten Jr, R. E. Activity metabolism of anuran amphibians: tolerance to dehydration. *Physiol. Zool.* **60**, 576-585 (1987).
91 Qiu, R. *et al.* Soil moisture dominates the variation of gross primary productivity during hot drought in drylands. *Sci. Total Environ.* **899**, 165686 (2023).
92 Janzen, D. H. & Schoener, T. W. Differences in insect abundance and diversity between wetter and drier sites during a tropical dry season. *Ecology* **49**, 96-110 (1968).
93 Tracy, C. R. *et al.* Thermal and hydric implications of diurnal activity by a small tropical frog during the dry season. *Austral. Ecol.* **38**, 476-483 (2013).
94 Forti, L. R., Hepp, F., de Souza, J. M., Protazio, A. & Szabo, J. K. Climate drives anuran breeding phenology in a continental perspective as revealed by citizen-collected data. *Divers. Distrib.* **28**, 2094-2109 (2022).
95 Walpole, A. A., Bowman, J., Tozer, D. C. & Badzinski, D. S. Community-level response to climate change: shifts in anuran calling phenology. *Herpetol. Conserv. Biol.* **7**, 249-257 (2012).
96 Miller, D. A. *et al.* Quantifying climate sensitivity and climate-driven change in North American amphibian communities. *Nat. Commun.* **9**, 3926 (2018).
97 Díaz-Paniagua, C. *et al.* Groundwater decline has negatively affected the well-preserved amphibian community of Doñana National Park (SW Spain). *Amphib-Reptilia* **1**, 1-13 (2024).
98 Seebacher, F., White, C. R. & Franklin, C. E. Physiological plasticity increases resilience of ectothermic animals to climate change. *Nat. Clim. Change* **5**, 61-66 (2015).
99 Wygoda, M. Adaptive control of water loss resistance in an arboreal frog. *Herpetologica* **44**, 251-257 (1988).
100 Riddell, E. A., Roback, E. Y., Wells, C. E., Zamudio, K. R. & Sears, M. W. Thermal cues drive plasticity of desiccation resistance in montane salamanders with implications for climate change. *Nat. Commun.* **10**, 4091 (2019).
101 Chown, S. L., Sørensen, J. G. & Terblanche, J. S. Water loss in insects: an environmental change perspective. *J. Insect Physiol.* **57**, 1070-1084 (2011).
102 Hoffmann, A., Hallas, R., Dean, J. & Schiffer, M. Low potential for climatic stress adaptation in a rainforest *Drosophila* species. *Science* **301**, 100-102 (2003).
103 Sheridan, J. A., Mendenhall, C. D. & Yambun, P. Frog body size responses to precipitation shift from resource-driven to desiccation-resistant as temperatures warm. *Ecol. Evol.* **12**, e9589 (2022).
104 Guo, C., Gao, S., Krzton, A. & Zhang, L. Geographic body size variation of a tropical anuran: effects of water deficit and precipitation seasonality on Asian common toad from southern Asia. *BMC Evol. Biol.* **19**, 1-11 (2019).
105 Castro, K. M. *et al.* Water constraints drive allometric patterns in the body shape of tree frogs. *Sci. Rep.* **11**, 1218 (2021).
106 Gouveia, S. F. *et al.* Biophysical modeling of water economy can explain geographic gradient of body size in anurans. *Am. Nat.* **193**, 51-58 (2019).
107 Daufresne, M., Lengfellner, K. & Sommer, U. Global warming benefits the small in aquatic ecosystems. *Proc. Natl. Acad. Sci.* **106**, 12788-12793 (2009).
108 Gardner, J. L., Peters, A., Kearney, M. R., Joseph, L. & Heinsohn, R. Declining body size: a third universal response to warming? *Trends Ecol. Evol.* **26**, 285-291 (2011).
109 Sheridan, J. A. & Bickford, D. Shrinking body size as an ecological response to climate change. *Nat. Clim. Change* **1**, 401-406 (2011).
110 Wu, N. C. & Seebacher, F. Bisphenols alter thermal responses and performance in zebrafish (*Danio rerio*). *Conserv. Physiol.* **9**, coaa138 (2021).
111 Kellermann, V., McEvey, S. F., Sgrò, C. M. & Hoffmann, A. A. Phenotypic plasticity for desiccation resistance, climate change, and future species distributions: will plasticity have much impact? *Am. Nat.* **196**, 306-315 (2020).
112 Gerick, A. A., Munshaw, R. G., Palen, W. J., Combes, S. A. & O'Regan, S. M. Thermal physiology and species distribution models reveal climate vulnerability of temperate amphibians. *J. Biogeogr.* **41**, 713-723 (2014).
113 Wu, Y. *et al.* Hydrological projections under CMIP5 and CMIP6: sources and magnitudes of uncertainty. *B. Am. Meterorol. Soc.* **105**, E59-E74 (2024).

Author contribution: NCW and CAN conceived the study, NCW and JDK compiled the data, RPB, CAN, and SCT provided additional unpublished data for 39 species, MRK and UEU developed the model simulations, NCW analysed the data, produced the figures, and wrote the initial draft. All authors contributed to the revisions.

Acknowledgements: This paper is dedicated to the late Professor Phillip J. Bishop (1957–2021) who was at the forefront of amphibian conservation research in the southern hemisphere. Phil dedicated more than 30 years to amphibian conservation and this study was inspired partly by his research

and his passion for amphibians at the Word Congress of Herpetology in Dunedin, New Zealand, 2020.

Competing interests: The authors declare no competing interests.

Funding information: UEU is financially supported by the Institute of Vertebrate Biology of the Czech Academy of Sciences (RVO: 68081766), RPB received financial support by the São Paulo Research Foundation—FAPESP (#10/20061-6, #14/05624-5, #17/10338-0, #19/04637-0). SCT's amphibian research was supported by the National Research Foundation of South Africa.

Data and Code Availability: Data and code to reproduce the study are available on the GitHub repository: https://github.com/nicholaswunz/global-frog-drought and will be available on Zenodo upon acceptance.

EXTENDED DATA

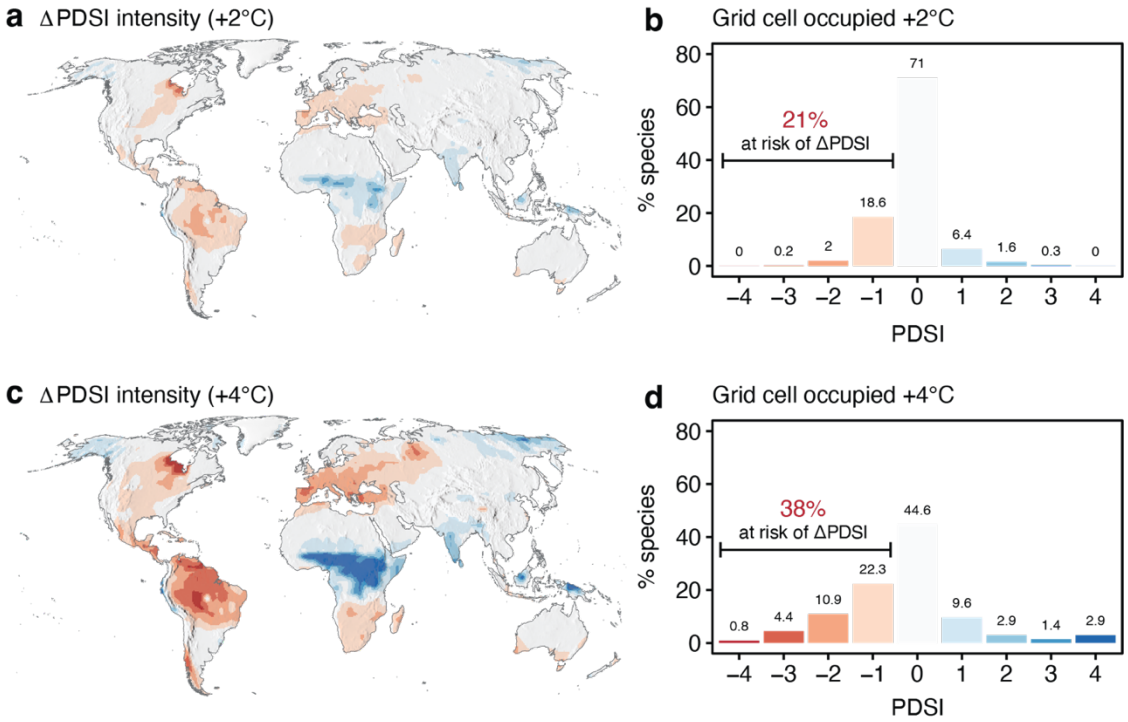

Extended Data Fig. 1 | Risk to increasing drought intensity for anurans by 2080–2100. (a) Change in the Palmer Drought Severity Index (ΔPDSI) under a +2°C warming scenario (Shared Socioeconomic Pathways 2–4.5; SPP2–4.5) by 2080–2100 relative to the current scenario (1970–1999). A decrease ΔPDSI indicates higher drought occurrences, while an increase ΔPDSI indicates more extreme wetness. (b) Percentage of anuran species occupancy in each PDSI category grid cell (0.5°) under a +2°C warming scenario, where 21% of species are in areas that are at risk of increasing drought. (c) Change in ΔPDSI under a +4°C warming scenario (SPP5–8.5). (d) Percentage of anuran species occupancy in each PDSI category grid cell (0.5°) under a +4°C warming scenario, where 38% of species are in areas that are at risk of increasing drought.

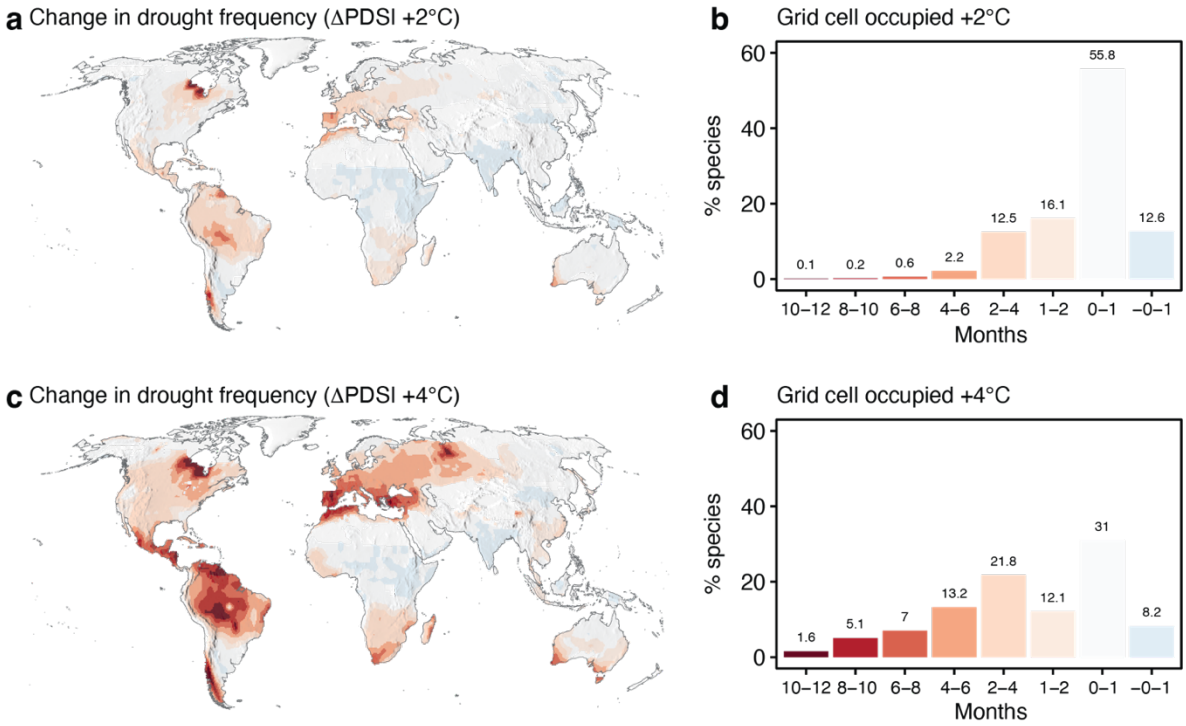

Extended Data Fig. 2 | Risk to increasing drought frequency for anurans by 2080–2100. (a) Change in the drought frequency ($\Delta PDSI_{[frequency]}$) under a +2°C warming scenario (Shared Socioeconomic Pathways 2–4.5; SPP2–4.5) by 2080–2100 relative to the current scenario (1970–1999). $\Delta PDSI_{[frequency]}$ was defined as change in monthly PDSI below -2 (moderate to extreme drought) within a 20 year period. **(b)** Percentage of anuran species occupancy in each frequency category grid cell (0.5°) under a +2°C warming scenario. **(c)** Change in the $\Delta PDSI_{[frequency]}$ under a +4°C warming scenario **(**SPP5–8.5**). (d)** Percentage of anuran species occupancy in each frequency category grid cell (0.5°) under a +4°C warming scenario.

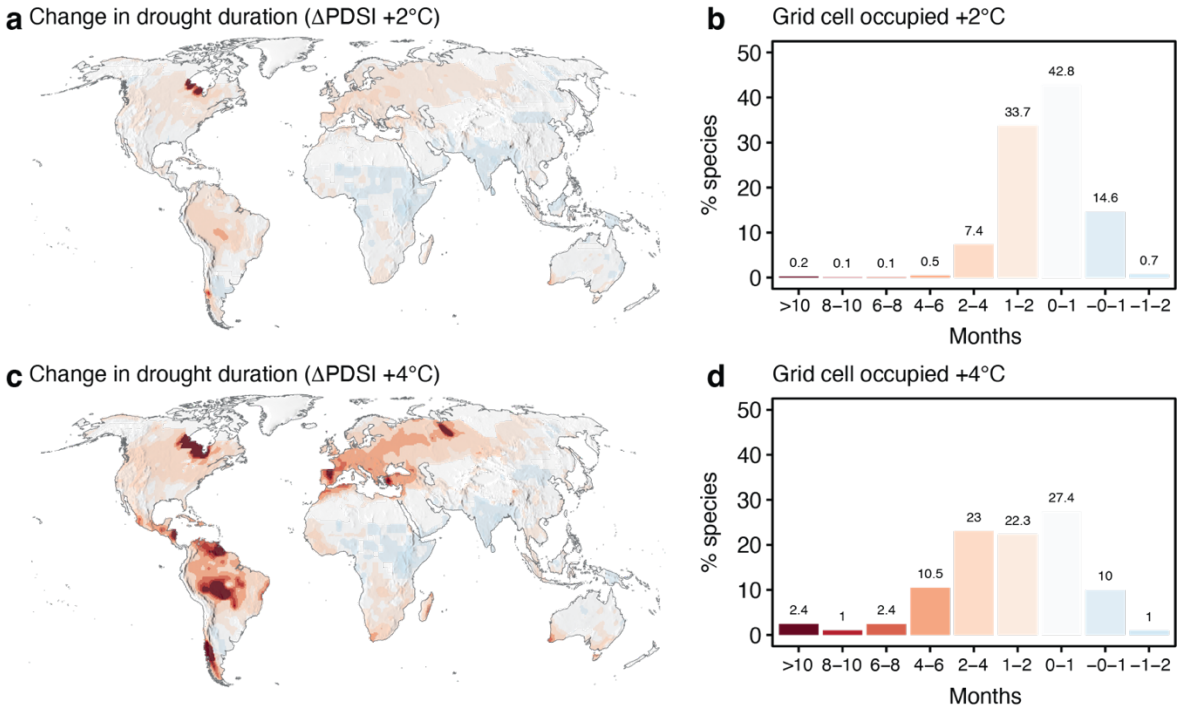

Extended Data Fig. 3 | Risk to increasing drought duration for anurans by 2080–2100. **(a)** Change in the drought duration ($\Delta PDSI_{[duration]}$) under a +2°C warming scenario (Shared Socioeconomic Pathways 2–4.5; SPP2–4.5) by 2080–2100 relative to the current scenario (1970–1999). $\Delta PDSI_{[duration]}$ was defined as consecutive months under moderate to extreme drought (PDSI < -2) within a 20 year period. **(b)** Percentage of anuran species occupancy in each duration category grid cell (0.5°) under a +2°C warming scenario. **(c)** Change in the $\Delta PDSI_{[duration]}$ under a +4°C warming scenario **(**SPP5–8.5**). (d)** Percentage of anuran species occupancy in each duration category grid cell (0.5°) under a +4°C warming scenario